Evaporation over land-surfaces: First results from HAPEX-MOBILHY special observing period

Jean-Claude Andre, Jean-Paul Goutorbe, Alain Perrier, François Becker, Pierre Bessemoulin, Philippe Bougeault, Yves Brunet, Wilfried Brutsaert, Tobby Carlson, Richard Cuenca, et al.

Evaporation over land-surfaces : First results from HAPEX-MOBILHY special observing period

Jean-Claude ANDRÉ [1], Jean-Paul GOUTORBE [1], Alain PERRIER [2]
François BECKER [3,4], Pierre BESSEMOULIN [1], Philippe BOUGEAULT [1],
Yves BRUNET [2], Wilfried BRUTSAERT [5], Tobby CARLSON [6],
Richard CUENCA [7], John GASH [8], Jacques GELPE [9], Peter HILDEBRAND [10],
Jean-Pierre LAGOUARDE [11], Colin LLOYD [8], Larry MAHRT [12],
Patrick MASCART [13], Christine MAZAUDIER [14], Joel NOILHAN [1],
Catherine OTTLÉ [14], Marc PAYEN [1], Thierry PHULPIN [1], Roland STULL [15],
James SHUTTLEWORTH [8], Thomas SCHMUGGE [16], Odile TACONET [14],
Catherine TARRIEU [1], Rose-May THEPENIER [1], Charles VALENCOGNE [17],
Daniel VIDAL-MADJAR [14], and Alain WEILL [14]

[1] *Centre National de Recherches Météorologiques (DMN/EERM),* 31057 *Toulouse Cedex, France*
[2] *Institut National de Recherches Agronomiques, Bioclimatologie,* 78850 *Grignon, France*
[3] *Groupement Scientifique de Télédétection Spatiale,* 67000 *Strasbourg, France*
[4] *NASA Goddard Space Flight Center, Greenbelt, Md* 20771, *USA*
[5] *School of Civil and Environmental Engineering, Cornell University, Ithaca, NY* 14853, *USA*
[6] *Department of Meteorology, Pennsylvania State University, University Park, Pa* 16802, *USA*
[7] *Department of Agricultural Engineering, Oregon State University, Corvallis, Or* 97331, *USA*
[8] *Institute of Hydrology, Wallingford, OX*10 8*BB, United Kingdom*
[9] *Institut National de Recherches Agronomiques, Pierroton,* 33610 *Cestas, France*
[10] *National Center for Atmospheric Research, Boulder, Co* 80307, *USA*
[11] *Institut National de Recherches Agronomiques, Bioclimatologie,* 84140 *Montfavet, France*
[12] *Department of Atmospheric Sciences, Oregon State University, Corvallis, Or* 97331, *USA*
[13] *Laboratoire Associé de Météorologie Physique,* 63000 *Aubière, France*
[14] *Centre de Recherches en Physique de l'Environnement, CNET/CNRS,* 92131 *Issy-les-Moulineaux, France*
[15] *Department of Meteorology, University of Wisconsin, Madison, Wc* 53706, *USA*
[16] *Hydrology Laboratory, US Department of Agriculture, Beltsville, Md* 20705, *USA*
[17] *Institut National de Recherches Agronomiques, Bioclimatologie,* 33140 *Pont de la Maye, France*

Received October 1, 1987 ; revised April 7, 1988 ; accepted April 15, 1988

ABSTRACT. The HAPEX-MOBILHY programme is directed at studying the hydrological budget and evaporation flux at the scale of a GCM grid square, i.e. 10^4 km^2. Different surface and subsurface networks were operated from mid-1985 to early-1987 to measure and monitor soil moisture, surface-energy budget and surface hydrology, as well as atmospheric properties.

A Special Observing Period (SOP) was organized from May 7 to July 15, 1986, and included detailed measurements of atmospheric fluxes and intensive remote-sensing of surface properties using two well-instrumented aircraft.

The first preliminary results from the SOP are presented. They concern mainly the intercomparison between various experimental systems and methods to estimate the local and/or area-averaged evaporation flux. It is shown that the measurements are reliable at the spatially local and short time scales, as well as at a much longer, i.e. monthly, time scale. These comparisons also include information retrieved from numerical simulations using mesoscale atmospheric models and data collected by airborne remote-sensing.

The complete database, against which parameterization schemes for land-surface water budget can be tested and developed, will be made available to interested scientists.

Annales Geophysicae, 1988, **6,** (5), 477-492.

1. INTRODUCTION

The HAPEX-MOBILHY (Hydrologic Atmospheric Pilot Experiment and Modélisation du Bilan Hydrique) programme (André *et al.*, 1986) is directed at studying the hydrological budget and evaporation fluxes at the scale of a General Circulation Model (GCM) grid square, i.e. of the order of 10^4 km^2. The many parameters that control the water budget and evaporation flux have very different time and spatial scales. As discussed in André *et al.* (1986), surface hydrology and upper soil properties have typical horizontal scales in the order of 100 m, while their time scales are relatively long, i.e. around 10 days. Accordingly, the year-round variations of such parameters have been monitored with a sampling interval in the order of 10 days and with many point measurements close enough to each other and in typical locations, in order to retrieve significant values. On the other hand, surface properties like temperature, surface eddy fluxes and other atmospheric boundary layer parameters vary on a fairly large spatial scale, close to 1 to 10 km, but have much shorter time scales, in the order of 1 h. The year-round variations of these quantities have consequently been monitored by instrumenting a regularly spaced surface network, but with a sampling interval in the order of only a few hours. These various networks are shown on figure 1, together with the geographical location of the experiment in southwest France (see André *et al.*, 1986, for more details). They were operated from April 1985 (surface hydrology and upper soil moisture content) or May 1986 (surface energy budget and surface heat fluxes) until mid-January 1987 (beginning of the winter period with saturated upper soil moisture and potential evaporation over bare soils).

Besides the above monitoring of surface, subsurface and atmospheric parameters, it was necessary to organize a Special Observing Period (SOP), the purpose of which was three-fold :

(i) aggregate the various point measurements taken during the year-round monitoring period, and particularly the turbulent sensible heat and evaporation fluxes, in order to provide an area-integrated value. This was achieved by flying the NCAR King-Air instrumented airplane (NCAR/RAF, 1984) over the entire surface network. The aggregation method to be developed from the SOP results will then be used to estimate the area-averaged evaporation flux from the individual spot measurements during the entire duration of the HAPEX-MOBILHY experiment ;

(ii) perform both more detailed and additional studies of rapidly varying, or difficult to measure, parameters, in order to compare the measurements given by the different sensors implemented in the surface networks with some kind of reference values. Such additional information has also proved of much help in documenting the various processes acting at the diurnal scale ;

(iii) conduct other complementary, or guest, studies which require either expensive equipment or considerable manpower. Airbone remote-sensing determination of surface parameters and budgets using the NASA C-130 instrumented airplane (NASA/AMES,

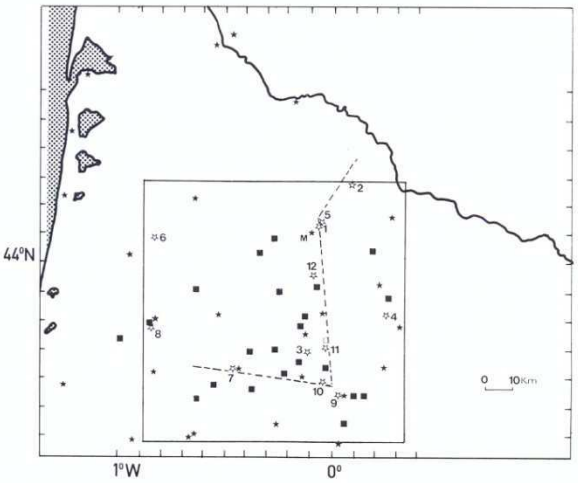

Figure 1

Site for the HAPEX-MOBILHY *experiment in southwest France, with location of the experimental sites (full star :* PATAC *station ; open star :* SAMER *station associated with neutron-sounding ; open square : neutron-sounding station ; full square : stream-gaging station ;* M : *forest mast). The solid line indicates the limits of the experimental zone, while the dashed line shows the track of the* NCAR *King-Air flux-measuring aircraft. The central site of Lubbon is located near sites* # 1 *and* 5 *and the forest mast, while the remote-sensing southern site of Castelnau is located at site* # 10.

1986) has been the most important of such complementary studies. It was especially aimed at providing a detailed ground truth to test and calibrate inversion methods to be applied to the satellite observations to be collected under the International Satellite Land-Surface Climatology Project (ISLSCP, see Bolle and Rasool, 1985).

The SOP started on May 7, 1986, at the beginning of the drying season in southwest France, and ended on July 15, 1986, at a time when the moisture content of the upper soil layers was down to approximately 1/3 of the field capacity. Besides their main use for the development of the previously mentioned aggregation method, data collected during the SOP will also be applied to the study of evaporation fluxes during such a climatologically important period, i.e. the depletion of surface moisture and subsequent stress on vegetation.

For the sake of completeness, it may be useful to briefly recall the major systems which have been implemented during the HAPEX-MOBILHY programme, and particularly during the SOP (see also André *et al.*, 1986) :

(i) in addition to the 2 stations of the Direction de la Météorologie Nationale (DMN) within the experimental domain of 10000 km^2, 5 others located close to its edges, 59 raingages and 19 stations measuring daily maximum and minimum temperature, the surface network further included : 19 automatic PATAC (SMIRSO, 1985) weather stations (a total of 42 PATAC stations cover most of southwest France) and 12 especially installed SAMER (Riou, 1982 ; Itier, 1982) stations for the measurement of the various components of the surface energy budget. Around

each of these 12 SAMER stations, and in 2 other locations of special interest, neutron-probe measurements of soil moisture variations were also performed ;

(ii) as almost 40 % of the experimental domain is covered by a fairly homogeneous pine forest, a site has been especially equipped for measurements within and above such tall canopies. An automatic weather station and a system for eddy-correlation measurement of the evaporation flux (Shuttleworth *et al.*, 1984) were mounted at the top of a mast. This forest site also includes neutron-sounding of soil moisture, measurement of radiative fluxes at the level of the undergrowth, and numerous raingages in order to estimate the interception losses of precipitation ;

(iii) the NCAR King-Air (NCAR/RAF, 1984), especially instrumented for the eddy-correlation measurement of evaporation and other turbulent fluxes, was flown approximately every third day at various levels within and immediately above the atmospheric boundary layer, including a systematic low level flight at 100 m to get the best possible estimate of the surface eddy fluxes ;

(iv) intensive radio-sounding of the atmospheric boundary layer, and more generally of the entire troposphere, was performed on special days, including all days when the King-Air was flying. Minimum time interval between soundings was 2 h, with soundings starting in the early morning and ending in the late afternoon in order to observe the daily variation of the moisture budget of the atmospheric boundary layer. These wind, temperature and humidity profiles were completed by systematic wind profiling of the lowest 500 m using acoustic sounders (Weill *et al.*, 1978). Both the radio-sounding station and the acoustic sounders were located in large clearings within the forest close to, or within, the central site, so that fluxes inferred from these measurements can be compared to other forest fluxes (see ii) ;

(v) the central site, installed within a large clearing close to the forest site, was further equipped with more sophisticated instruments. These special systems, including a 12 m meteorological mast instrumented with anemometers and temperature sensors at 8 levels, another mast for humidity measurements, a strain-gage weighing lysimeter, and a BEARN system (Perrier *et al.*, 1975) based on the Bowen ratio technique, gave access to more precise estimations of the local evaporation flux and are used for intercomparison purposes ;

(vi) tropospheric radio-soundings were launched daily at 6 h intervals at the central site (see iv), Bordeaux and Toulouse. Caging flights by 2 smaller airplanes at 2 levels around the experimental square (one within the boundary layer and the other one just above it) were operated by the Centre d'Aviation Météorologique (CAM) on selected days. Together with these aircraft data and the measurements from the various instruments in the surface network, the frequent radio-soundings provided a wealth of information at the mesoscale, against which it is possible to test and validate three-dimensional atmospheric mesoscale models. These numerical mesoscale models are indeed thought to be an essential tool for the development of an aggregation method for the determination of area-averaged fluxes from point measurements (André and Bougeault, 1987) ;

(vii) airborne remote-sensing of land-surface parameters was performed by the NASA C-130 instrumented airplane (NASA/AMES, 1986), with special emphasis on the central site and on a secondary, more southerly, site, where additional ground-truth measurements relative to vegetation processes were undertaken.

The main purpose of this paper is to present the first results from the SOP. Such results concern mainly the intercomparison between various experimental systems and methods to estimate the local and/or area-averaged evaporation flux. Some available preliminary results on local surface budgets will also be shown, including comparison with outputs from numerical mesoscale three-dimensional atmospheric models.

2. THE SAMPLING OF SURFACE FLUXES FROM MESOSCALE NETWORKS

2.1. The various instruments

Each SAMER (Système Automatique de Mesure de l'Evapotranspiration Réelle) station includes a radiation budget meter for both short-wave and long-wave upward and downward components, a net radiometer and a flux-meter measuring the heat flux G in the ground. The temperature and wind velocity gradients between two levels are sampled. The sensible heat flux H is retrieved *via* a flux-gradient relationship, and the evaporation flux LE by balancing the surface energy budget

$$LE = R_N - G - H \,. \qquad (1)$$

This system also collects conventional temperature and humidity data at screen height and includes a recording raingage. In order to monitor the local water budget, neutron-probe measurements of soil moisture were made around each SAMER station every week. A brief description of the various sites, shown in figure 1, is given in table 1. This system was fully operational at the end of May, 1986 and information was sent *via* telephone lines to a data collection computer in Toulouse until January, 1987.

In contrast to these rather long term operations, two sites were equipped more thoroughly during the SOP. Both were used as test sites for aircraft remote-sensing studies (see Section 6). The so-called central site in Lubbon (sites # 1 and 5) is a large clearing in the northern pine forest. It is a large $(2\ \mathrm{km})^2$ plot of sandy soil, artificially drained and cultivated. The two crops grown there are grain corn, which was irrigated after the end of the SOP, and oats. Evaporation over a developing oat field was measured using several systems (see Section 1), including a SAMER station and neutron-probe access tubes, so that various ways of estimating or measuring evapotranspiration can be compared at this site.

Table 1

Location of the sites with surface energy and moisture budgets measurements, with indication of pedological and agricultural conditions. The moisture depletion Δm is measured by neutron-sounding down to the indicated depth, P is the amount of precipitation and E is the amount of evaporation as measured by the SAMER *station. The imbalance $Y = -\Delta m + P - E$ is expressed in* mm *or as a fraction of $(P - \Delta m)$.*

Site #	Location	Type of soil	Type of crop	Depth of measurements (m)	Period of investigation	Δm moisture depletion (mm)	P precipitation (mm)	E evaporation (mm)	Y imbalance (mm)	(%)
1	Lubbon 1	Sand	oats	1.6	6/3-7/16	− 90	42	116	16	12
2	Casteljaloux	Silty clay	corn	1.6	5/26-7/1	− 57	19	80	− 4	5
3	Caumont	Sandy clay loam	soya	1.6	5/28-7/18	− 123	54	178	− 1	0
4	Courrensan	Clay and limestone	wheat	1.5	5/15-7/17	− 79	37	123	− 7	6
5	Lubbon 2	Sand	corn	0.7	5/13-6/24	− 93	52	129	16	11
6	Sabres	Sand	corn	1.6	5/20-6/16	− 38	30	70	− 2	3
7	Bats	Clay loam	corn	1.6	5/27-7/17	− 85	46	140	− 9	7
8	Vicq	Loamy sand	corn	2.0	6/2-6/30	− 15	67	88	− 6	7
9	Tieste	Sandy clay loam	corn	0.9	6/4-7/19	− 19	75	142	− 48	51
10	Castelnau	Sandy clay loam	corn	1.7	5/29-7/18	− 73	60	132	1	0
11	Fusterouau	Sandy clay loam	corn	1.7	6/4-7/19	− 33	83	115	1	0
12	Lagrange	Sandy clay loam	corn	1.8	6/11-7/17	− 41	20	84	23	37

A secondary test site, very different from the first one, was set up at Castelnau, in the southern part of the network and located on a plateau on the left bank of the Adour river (site # 10). In addition to a SAMER station, a plot of grain corn was equipped with a 15 m mast instrumented at 6 levels with ventilated copper-constantan thermocouples as temperature sensors and count anemometers as wind velocity sensors. Wet bulb temperature was also measured at the height of 2.3 m. The soil temperature profile was determined with 7 thermocouples between 2 cm and 1 m below the soil surface. A Thornthwaite heat flux plate measured the heat flux into the ground at a depth of 2 cm. The neutron-probe system was augmented by performing measurements of soil water tension at different depths. On a few days eddy-correlation measurements were also performed.

2.2. Comparisons between the various ground-based measurements of the evaporation flux

Comparisons between estimates of the sensible heat flux H from SAMER and BEARN (Bilan d'Energie Automatique Régional et Numérique) systems over site # 1 are shown in figure 2. It must first be emphasized that these two estimates are based on rather different techniques. For the SAMER, H is computed from wind speed and temperature differences at two levels using a simplified aerodynamic formula, therefore making no use of the net radiation at the surface. For the BEARN, H is deduced from the net radiative flux (minus the heat flux into the ground) by using a Bowen ratio assumption. In figure 2*a* the oats, over which the measurements were taken, were in an active growth stage (May 22, 1986), so that the sensible heat flux is quite small as compared to the available radiative energy. Most of the available energy is released to the atmosphere as latent heat flux caused by canopy evapotranspiration. One striking feature appearing in figure 2*a* is the occurrence of a negative sensible heat flux after midday. It can be explained by the fact that at this time of year the other fields around the oats were still bare soil, as corn and other crops were not growing as rapidly as the oats. Oats were consequently transpiring at a much higher rate than the surroundings, giving rise, through the well-known oasis effect, to a deficit in sensible heat balanced by local advection from the surrounding bare-soil plots. Approximately one month later (June 28, 1986), the oats were very close to full maturity and were transpiring at a much lower rate (fig. 2*b*). The sensible heat flux is then much closer to the available radiative energy, especially by the end of the afternoon when the canopy water stress is a maximum. The difference which can be seen in

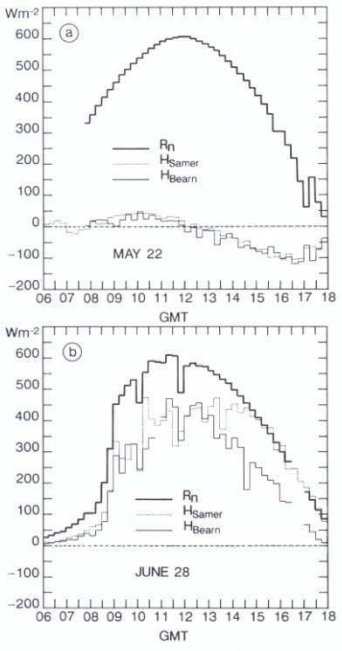

Figure 2

Comparison between surface fluxes H of sensible heat observed at Lubbon over oats (site # 1) by the SAMER *(dotted line) and the* BEARN *(solid line) systems for (a) May 22 and (b) June 28, 1986. The heavy line shows the net radiative flux at the surface.*

figure 2*b* between SAMER and BEARN estimates after 14 GMT can be ascribed to different degrees in maturity of the oats over the two spots where the different measurements were made, 100 m apart from each other. This can be verified by the fact (not shown here) that on the following days the two SAMER and BEARN curves became again very close to each other, as the oats over the two spots reached full and complete maturity. It should however be mentioned here that changing wind direction led to different fetches for both instruments, so that part of the differences between fluxes from the SAMER and the BEARN seen in figure 2*b* in the late afternoon could be due to this effect. These sets of curves for the diurnal variation of the sensible heat flux H clearly indicate a strong consistency between the simplified SAMER measurements and more sophisticated ones.

Similar comparisons between SAMER and mast measurements are shown in figures 3*a* and 3*b*. The comparisons are made for a parcel of bare soil partly covered with young corn of 10 cm or so, at the site of Castelnau (site # 10). Although quite small, the fluxes are slightly different in the early morning. Discrepancies between half-hourly estimates of the sensible and latent heat fluxes are however smaller during midday, in the order of 10 %. One can further note that the overall diurnal variation of H and LE is the same as measured by the two systems.

Based on studies of the surface-energy budget, the SAMER system is therefore shown to produce accurate measurements of the evaporation flux at the short, i.e. hourly, time scale. From the above comparisons, and other studies not reported here, the overall accuracy of the SAMER measurements is in the order of 20 % for fluxes estimated over 15 min time interval. The accuracy of SAMER measurements appears to be much less for longer time-averaging, i.e. daily to monthly time scales. To show this, it is necessary to check the reliability of the SAMER measurements on a rather longer time scale, i.e. the weekly to monthly time scale characteristic of the surface hydrology budget.

Neutron-probe measurements of soil moisture content were made around each SAMER station on a weekly basis beginning in April, 1985. Each of these sites was equipped with 4 access tubes and neutron-probe readings were made from the surface down to a depth in the order of 1.5 m, with a vertical resolution equal to 0.1 m. The calibration coefficients were obtained by neutron absorption/diffusion analysis and adjusted using field data from each site. The types of soil and crop grown during the SOP are given in table 1. These soil moisture measurements can be used, together with the SAMER values for the evaporation flux E, to evaluate the various terms of the local hydrologic budget

$$\Delta m = P - E - Y\,, \qquad (2)$$

where Δm represents the variation of the soil-moisture content during a given time interval as derived from the evolution of the vertical soil-moisture profile. P and E are the amount of precipitation and evaporation measured respectively by raingages and SAMER stations during this same time interval. Eq. (2) ideally

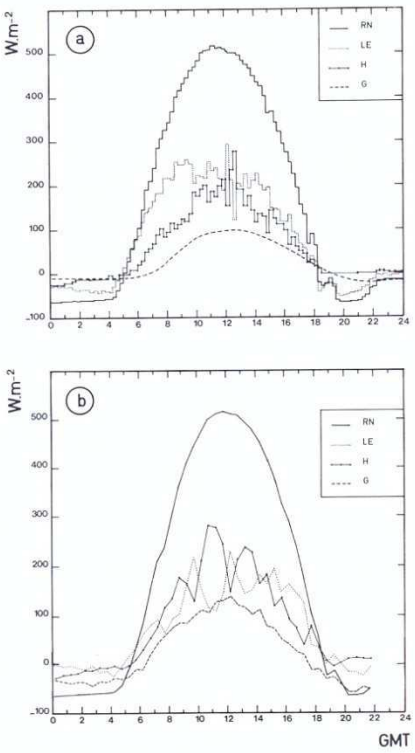

Figure 3
Comparison between surface fluxes at Castelnau over corn (site # 10) as observed from (a) the SAMER *station and (b) a mast-borne aerodynamic method, for June* 16, 1986.

suggests that a positive value of residual Y corresponds to surface and/or subsurface runoff, while a negative value of Y could account for lateral and/or upward supply of water. Of course, errors in the estimates of Δm, P, and E also contribute to the residual Y. Values of these three quantities are given in table 1 for a time interval of one month or so. Sites 2, 3, 4, 6, 7, 8, 10 and 11 are characterized by very low values of Y, less than 10 % of $(\Delta m - P)$. Higher and positive values of Y at sites 1 and 5 are probably due to the subsidence of the water table at the end of the SOP, resulting in an overestimation of Δm. This is confirmed by the time evolution of the vertical profiles of the volumetric moisture content at the central site (site # 1) shown in figure 4, where a sudden decrease of the water content occurs at a depth of 1.3 m in less than one week at the beginning of July. One can also notice in figure 4 that, starting from saturation in early May, soil moisture decreased steadily due to the development of the rooting system from mid-May to late June, while significant recharge occurred in the upper 0.8 m during the last 10 days of the SOP due to storms passing over the experimental zone on July 2, 6 and 12. Other large imbalances in the hydrological budget can be noticed for sites # 9 and # 12, the former being possibly due to lateral water supply, while the latter being possibly ascribed to the gentle slope running from a neighbouring plateau to the station. Such possible explanations for the anomalies in the local water budget will be checked when the simulations from the hydrological model of Girard and Boukerma (1985) are available for the catchments

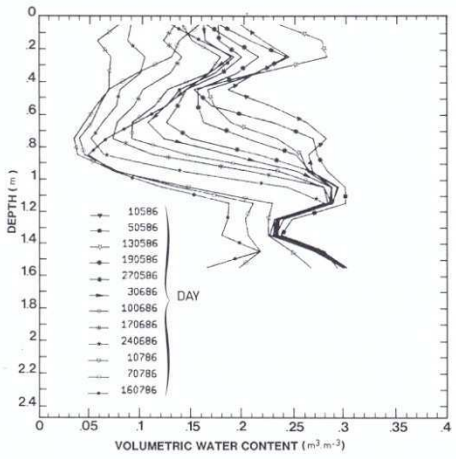

Figure 4

Time variation of vertical profiles of soil moisture content at the central site of Lubbon (sites # 1 and 5), as measured from neutron-sounding, for the period May 1 to July 16, 1986. One can note the progressive deepening of the rooting zone, as well as the collapse of the ground water table between July 1 and 7.

of interest. It can nevertheless be concluded from inspection of most of the data shown in table 1 that the SAMER measurements of the evaporation flux E are reliable at the monthly time scale, and do not exhibit systematic bias.

2.3. Spatial variability of surface fluxes

The spatial variability of evaporation fluxes, which is one of the essential features to be captured during the HAPEX-MOBILHY programme, may be due to either different climatic, hydrologic and/or pedologic conditions or to different vegetative canopies. It can be documented by either the surface network of SAMER stations or by aircraft measurements.

In figure 5*a* are shown the sensible heat flux variations during a typical fair-weather day (June 16, 1986) over oats (site # 1) and corn (site # 5) at two very close locations within the central site, i.e. for the same, or almost the same, climatic, hydrologic and pedologic conditions. It can be noted that the sensible heat flux over oats is significantly smaller than that over the corn. This is indicative that the oats are close to full maturity and consequently transpire and evaporate at a much higher rate than the corn which, for that time of year, is just starting to grow and still exhibits a large fraction of bare soil between the young plants. On the other hand, figure 5*b* shows, for this same day, the diurnal evolution of the sensible heat flux over the corn approximately 10 cm high, but for two different locations, one over sandy soil with moisture content close to 50 % of the saturation value (site # 8) and the other one over clay loam with lower moisture content, approximately 1/3 of the saturation value (site # 10). One can notice significant differences in heat fluxes due to the influence of varying hydrologic and pedologic conditions. The dryer, loamy soil gives rise to larger heat restitution to the atmosphere as compared to the moister sand.

The influence of different conditions and vegetative canopies on heat fluxes H and LE will be further shown using the NCAR King-Air measurements in Section 4.2, with special emphasis given to the influence of the relatively rough pine forest part of the experimental zone.

3. FLUXES OVER THE FOREST

3.1. The forest site and the various instrumental systems

The forest site is located very close to the central site of Lubbon (sites # 1 and # 5), north-east of the geographical center of the experimental zone. The area is almost flat and close to the water divide between the Garonne and the Adour river basins. An impervious layer exists at some variable depth and a shallow water table persists during most of the year (see e.g. fig. 4). The vegetation at and around the forest site is predominantly maritime pine trees with a density of about 430 trees per hectare and a mean height of 20 m, with a sub-canopy of bracken.

A 25 m high tower was instrumented with two automatic weather stations and, during the SOP, with eddy-correlation and radiation instrumentation. The evaporation of intercepted rainfall was deduced from measurements of gross rainfall and throughfall and stemflow. In addition soil moisture changes were monitored using a neutron moisture meter and a dense network of 12 access tubes. The transpiration from 10 trees was also measured using a heat pulse technique to monitor the sap flux.

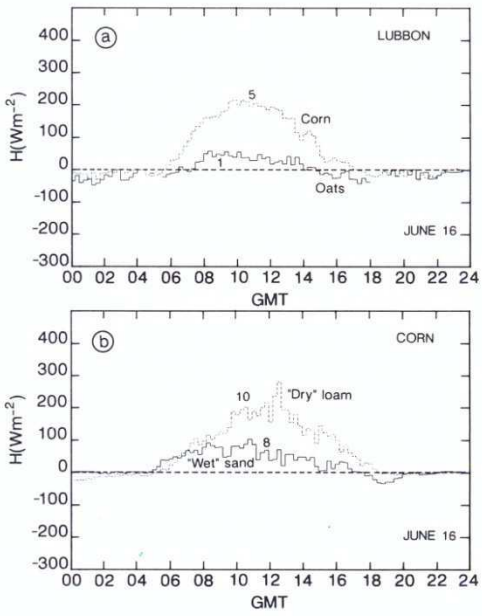

Figure 5

Comparison between surface fluxes H of sensible heat at different sites as measured from the SAMER *stations : (a) fluxes at Lubbon over oats (site # 1, solid line) and over corn (site # 5, dotted line) for June 16, 1986 ; (b) fluxes over corn grown on wet sandy soil (Vicq, site # 8, solid line) and on dry loam (Castelnau, site # 10, dotted line) also for June 16, 1986.*

The eddy-correlation system, an Institute of Hydrology Mk2 Hydra, comprised a vertical sonic anemometer, an infra-red hygrometer, and a fine-wire thermocouple. This instrument is an improved version of the Mk1 Hydra used by Shuttleworth *et al.* (1984) and Gash (1986). The fluxes are calculated on-line using a system similar to the one described by Lloyd *et al.* (1984).

3.2. First results

The radiation components for a typical day (June 16, 1986) are shown in figure 6. The sparse forest acts as an efficient radiation trap, with only some 10 % of the incident solar radiation being reflected back to the atmosphere. Approximately 30 % of the above canopy net radiation penetrates the tree canopy and is available for evaporation by the bracken sub-canopy or the forest floor. Figure 7 shows the partition of energy between evaporation and sensible heat flux as given by the eddy-correlation system. The average net radiation over the 24-h period was 223 W m^{-2}. During the same period the eddy-correlation system measured an average 115 W m^{-2} of evaporation and 110 W m^{-2} sensible heat flux. If the minor terms in the energy balance eq. (1) are neglected or assumed to cancel over the day, these figures imply a very good balance (the recovery ratio turns out to be 101 %). The Bowen ratio for these daily average fluxes is large (see fig. 4), so that despite this ready supply of soil water the evaporation was restricted by stomatal control.

3.3. Clearing *versus* forest fluxes

As already described in Section 2.1, a large clearing, where sites # 1 and # 5 were set up, is located in the north-east part of the pine forest, close to the forest site where measurements described in the preceding Section were taken. It is also from this Lubbon clearing that the frequent radio-sounding were launched.

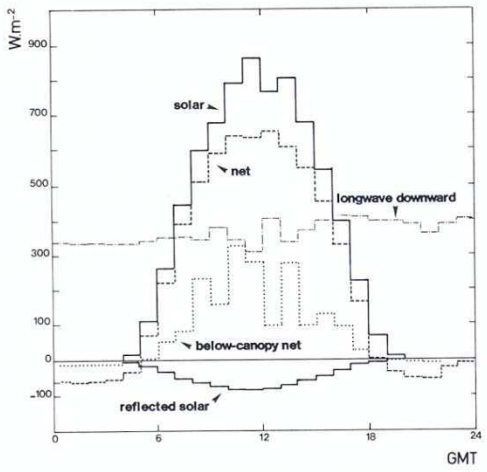

Figure 6
Radiation components for the forest site of Estampon on June 16, 1986.

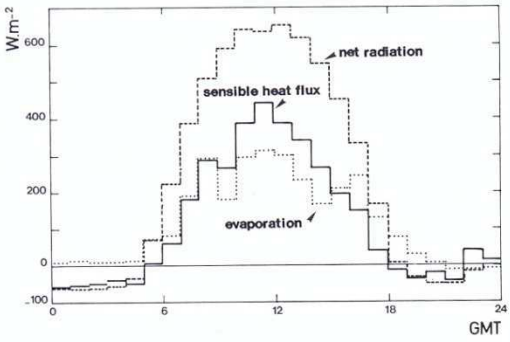

Figure 7
Surface energy partition for the forest site of Estampon on June 16, 1986, *derived from eddy-correlation and radiative measurements.*

These radio-sounding profiles of wind, temperature and humidity can be used to retrieve surface fluxes H and LE from the heat and moisture budgets of the planetary boundary layer. One can vertically integrate the equation for the rate of change of temperature between the surface $z = 0$ and the top of the boundary layer $z = h$ and, by assuming horizontal homogeneity of the turbulence and vanishing eddy fluxes at h, one gets

$$H = \int_0^h \mathrm{d}\theta/\mathrm{d}t \, \mathrm{d}z + \int_0^h \mathbf{v}_H \cdot \mathbf{grad}_H \, \theta \, \mathrm{d}z + \int_0^h w \, \mathrm{d}\theta/\mathrm{d}z \, \mathrm{d}z \quad (3)$$

where w is the vertical velocity and $\mathbf{v}_H$ the horizontal wind vector within the boundary layer. From successive radio-soundings taken every other hour or so, it is easy to estimate the first term in the right-hand side of eq. (3). The second and third terms of the right-hand side are estimated from the especially improved weather analysis maps which have been prepared using all the additional meteorological data collected daily during the SOP (see Section 5.2, for more detail). For the case of June 16, 1986, which is presented below, the vertical advection (last term of eq. (3)) has been neglected. Results are shown in table 2, where they are further compared to the flux estimates made from the other instruments installed in the immediate vicinity, i.e. the SAMER stations of sites # 1 and # 5 and the Hydra system in the forest site. It can first be noticed that the daily-average surface sensible heat flux H necessary to balance the heat budget eq. (3) of the planetary boundary layer compares quantitatively very well with the one measured over the forest by the Hydra system. This almost perfect quantitative agreement may of course be coincidental, as there may be rather large uncertainty in the measurement of the boundary-layer heat budget, but the daily variation of H as inferred from these two systems appears consistent, giving then more credence to the budget method. A second important feature appearing in table 2 is that the budget and Hydra fluxes over the forest differ very significantly from the ones estimated from the SAMER stations over oats or corn in the Lubbon

Table 2

Surface fluxes of sensible heat H over the central site on June 16, 1986, *as estimated from the* PBL *heat budget method, from* SAMER *measurements over oats or corn in a clearing, and from* Hydra *eddy-correlation measurements over the forest.*

Time interval (GMT)	PBL heat content variation (W m^{-2})	PBL heat advection (W m^{-2})	Surface heat flux H (W m^{-2}) from PBL heat budget	Surface heat flux H (W m^{-2}) over oats (site # 1)	Surface heat flux H (W m^{-2}) over corn (site # 5)	Surface heat flux H (W m^{-2}) over over the forest
05:21 - 07:57	72	73	145	−6	43	90
07:57 - 09:38	201	66	267	45	153	273
09:38 - 11:22	163	84	247	40	194	371
11:22 - 13:37	353	85	438	30	173	387
13:37 - 15:32	213	54	267	8	91	259
15:32 - 17:18	85	20	105	− 18	22	139
Total (kJ m^{-2}) 05:21 - 17:18	7 779	2 795	10 574	650	4 709	10 618
Mean values (Wm^{-2}) (05:21 - 17:18)	181	65	246	15	109	247

clearing. The much larger sensible heat fluxes over the forest as compared to the ones measured over crops in the clearing indicate that the forest has a much larger stomatal resistance than the growing agricultural canopies, as noted in the preceding Section.

The fact that the boundary layer reacts more to the fluxes over the forest than to the ones over the cultivated large clearings is further evidenced from low-level wind profiles taken by sodars. The Doppler sodars installed in the clearing at Lubbon and in the forest close to the Hydra tower provided raw data every 4 or 8 s with a vertical resolution varying between 4 and 17 m depending upon the particular sodar under consideration (see Weill *et al.*, 1978). These data have been processed to provide 20-min average wind profiles. Such profiles are shown in figure 8*a* for the forest, where one can note a good fit with the logarithmic law profile (the correlation coefficient between the data and the logarithmic fit shown in fig. 8*a* is equal to 0.82). The influence of the forest introduces a displacement height approximately equal to the height of the trees. On the contrary, wind profiles over the clearing (see fig. 8*b*), exhibit a more complex structure, with an almost linear variation of wind speed with altitude above 90 m, i.e. much higher than the top of the trees. Below this height the wind speed variations with height are less marked, with a tendency for higher winds as compared to the forest, possibly accounting for smaller roughness-induced surface drag. Further sodar data processing along the lines defined by Weill *et al.* (1980) should provide complementary estimates of momentum and sensible heat fluxes, which will then be compared to the other estimates available over the forest.

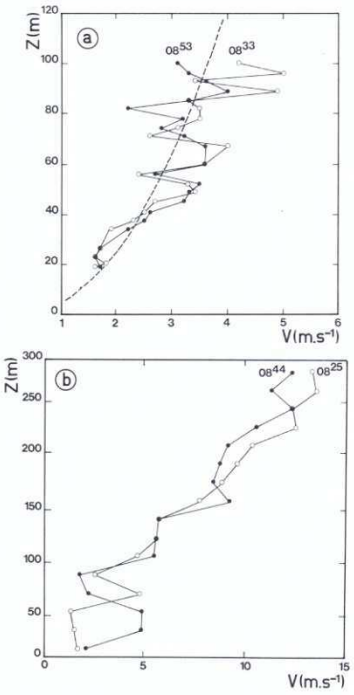

Figure 8

Vertical profiles of wind speed as measured by Doppler sodars on June 16, 1986, *at (a) the site of Estampon near the forest tower, and (b) the central site in Lubbon's clearing (sites # 1 and* 5).

4. AIRPLANE MEASUREMENTS OF AREA-AVERAGED FLUXES

As shown in the preceding Section, some systems provide measurements which are already spatially averaged, as is the case for the budget method and for the sodar estimates. However, the essential instrument for estimating the area-averaged fluxes is the instrumented King-Air aircraft (NCAR/RAF, 1984). The primary goal of King-Air participation in HAPEX-MOBILHY was measurement of the large-scale variability of surface fluxes H and LE. The aircraft measurements included observation of the variations in surface fluxes which were due to inhomogeneities in terrain, vegetation and soil type, as well as the seasonal variations of these fluxes during the drying SOP.

4.1. Data collection and processing

The King-Air capabilities include measurement of turbulent fluctuations of wind, temperature and humi-

dity. Turbulence intensities and fluxes of heat and momentum can be calculated from these measurements. In addition, the aircraft measures solar and terrestrial radiation, earth surface temperature, and aircraft height above terrain.

The 150 km flight track (shown on fig. 1) included a southern region of regular north-south hills, a central region of irregular small hills, and a flat forested region to the north. On each research day the full 150 km flight track was flown three times at an altitude of 100 m above hill tops. This low level data collection was designed to provide measurement of surface fluxes of heat and momentum. In addition, portions of the flight track were flown at 0.7-0.9 h and 0.4 h, where h is the planetary boundary-layer depth. These higher flight levels were designed to provide estimates of vertical flux gradients in the boundary layer.

The measurements were designed to evaluate surface layer turbulence and fluxes every 10 km along the 150 km flight track. Filtering techniques were used to remove large scale variations from the data, and the resulting turbulent fluctuations were averaged on a 10 km scale. Since the boundary layer was typically 0.7 to 1.0 km deep, the 10 km averaging length covered about 6 to 9 boundary-layer large eddies. A 5 km flux calculation scale was evaluated and rejected due to the noticeably increased scatter in those values. The large-scale fluctuations, removed during the filtering process, were used to evaluate large scale gradients in wind, temperature and humidity. Profiles of wind, temperature, humidity, momentum and heat fluxes show typical boundary-layer forms and illustrate that the scatter in the data is comparable to other similarly instrumented experiments. The flux profiles which can be derived from these data appear adequate for extrapolating the 100 m agl data to the ground for surface heat flux estimation.

4.2. Results and intercomparisons for area-averaged fluxes

The data for the fair-weather day June 16, 1986, are shown in figure 9 for 100 m agl eddy-kinetic energy, sensible and latent heat fluxes. These data show good agreement between the 10 km measurement points, thus indicating reasonably stable turbulence estimates on the 10 km scale. An increase in the magnitude of the eddy-kinetic energy and sensible heat flux can be seen with time of day, as can be expected for a typical convective boundary layer. A similar result is not seen in the latent heat flux values, possibly due to the larger scatter.

The eddy-kinetic energy and sensible heat flux have distinct peaks over the forested area. An increase in the momentum flux values was also noted over the forest (see Section 3.3, for independent confirmation). In relative contrast, the latent heat flux trace in figure 9 shows much smaller differences between the forested area and the central and southern agricultural areas. The turbulence, momentum and sensible heat fluxes increases over the forest seem related to the rougher forest surface and to the more efficient transfer of net radiation into sensible heat flux over

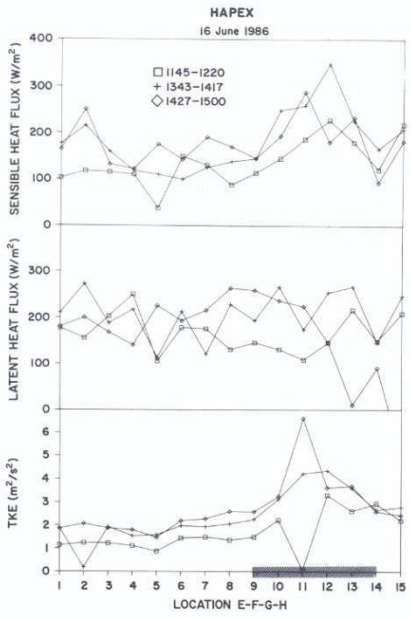

Figure 9
King-Air aircraft measurements of sensible heat flux H, latent heat flux LE, and eddy-kinetic energy K, for June 16, 1986. *Each measurement consists of the average over a* 10 km *segment and the* 15 *segments form the full* 150 km *flight track (see fig.* 1). *The hatched area between segments* 9 *and* 14 *corresponds to the location of the forest.*

the forest surface, as compared with agricultural areas. In contrast, even though the forest soil was still humid at the time of these measurements (see fig. 4) and the atmospheric turbulence intensities and transports were enhanced, the forest was not releasing water into the atmosphere at a faster rate than the agricultural areas in the center and the south of the research zone, as already discussed in Section 3.2.

It is of interest to compare the 10 km averaged values of surface fluxes given by the airplane measurements to the estimates from the instruments and systems implemented in the surface network. This is done in table 3 for June 16, 1986, where King-Air flux values for a given 10 km segment are compared to the values from the closest SAMER or Hydra stations. This comparison shows a good qualitative agreement, especially in the southern part of the research area (sites # 7, # 10 and # 11). There are quantitative differences between the SAMER and aircraft estimates, the latter being usually smaller than the former. Part or all of these differences may possibly represent the effect of spatial integration, which was the specific objective of the airplane participation. It must also be kept in mind that comparing 45-min averaged values as done in table 3 may well induce more scatter than would otherwise appear when dealing with daily averages. The lower values of aircraft latent heat flux LE are to be particularly noticed for the flight segments over the forest and clearing sites, but it can be seen from figure 9 that the spatial variation of latent heat flux in this area is the largest as compared to other parts of the experimental zone. This calls for refined aircraft data processing,

Table 3

Surface fluxes of latent heat LE over various sites as measured by the surface stations (SAMER *and Hydra*) *and by airborne eddy-correlation technique. The first number refers to measurements made between* 09:30 *and* 10:15 GMT, *while the second one corresponds to measurements made between* 12 :15 *and* 13:00 GMT.

Site #	Location	SAMER or Hydra latent heat fluxes (W m^{-2})	King Air latent heat fluxes (W m^{-2})
7	Bats	165/245	185/175
10	Castelnau	230/180	130/210
11	Fusterouau	215/180	170/195
12	Lagrange	225/180	150/255
5	Lubbon (corn at the central site)	340/420	120/190
—	Estampon (forest at the central site)	235/297	

particularly for fluctuating humidity as measured from the airborne Lyman-hygrometers (see Stull, 1985).

5. USING ATMOSPHERIC MESOSCALE MODELLING FOR SPATIAL INTEGRATION OF SURFACE PROPERTIES AND FLUXES

In order to take full advantage of the spatial coverage of the experimental network, and to address specifically the problem of determining effective evaporation fluxes over a GCM grid square with varying surface and subsurface conditions, a strategy has been developed, based on the use of mesoscale modelling (André and Bougeault, 1987).

5.1. The modelling strategy

It is deyeloped by following five main steps :

(*i*) obtain the best possible mesoscale meteorological analysis by use of the higher-frequency radio-sounding network and of objective analysis and model assimilation techniques similar to those used for operational weather forecasting (see below Section 5.2) ;

(*ii*) use the so-obtained analysis as atmospheric forcing to calibrate by trial-and-error the physical packages of the three-dimensional numerical mesoscale models. This is to be done by column-model integration and comparison of the results with the measurements of the SAMER and the Hydra systems, allowing for the determination of the adjustable parameters of the physical packages from the local physical properties (soil and vegetation type, etc.) ;

(*iii*) derive spatial fields of these same parameters from satellite products, or other already existing information like maps of soil properties and/or vegetation cover. At this stage there is of course some uncertainty on the precise physical meaning of some of these parameters, such as the vegetation index, but such ambiguity might be resolved by the further steps ;

(*iv*) implement the three-dimensional models with varying surface characteristics, as determined by the maps obtained from step (*iii*), and estimate from the three-dimensional model integrations the spatially-averaged evaporation fluxes. At this stage it is necessary to assess by any possible means the validity of the three-dimensional simulations ;

(*v*) compare the three-dimensional model results with the aircraft measurements, which are themselves spatially averaged over 10 km, and reconsider if necessary the correspondence between local values of the adjustable parameters obtained at step (*ii*) and integrated values obtained at step (*iii*). This has to be repeated by a trial-and-error procedure until the results of the three-dimensional models have achieved the highest degree of realism.

5.2. Improvement of the atmospheric analysis

The Direction de la Météorologie Nationale (DMN) is using for operations an objective analysis programme based on the optimum interpolation technique (Durand, 1985). This analysis method provides fields of surface pressure and atmospheric variables (horizontal wind, temperature and humidity) at 15 levels between the ground and the top of the atmosphere. The horizontal spatial resolution is typically 100 km, while the vertical one is of the order of the boundary-layer depth close to the ground.

During the SOP the radio-soundings stations of Bordeaux (50 km north-west of the experimental zone), Toulouse (100 km to the east of the experimental zone) and Lubbon (central site) increased the frequency of launches to at least 4 soundings per day (00, 06, 12 and 18 GMT). Using this wealth of additional data on the atmospheric structure, the analysis programme has been run 4 times a day, providing a detailed picture of the atmospheric structure (Mercusot *et al.*, 1986) in a format ready for model studies, or for other types of studies like the budget analysis described in Section 3.3.

5.3. First results from mesoscale modelling

Numerical experiments have been undertaken with two three-dimensional models. Those are the DMN's limited-area model PERIDOT (Prévision à Echéance Rapprochée Incluant des Données d'Observation Télédétectées) (Imbard *et al.*, 1986) specially operated at the meso-β-scale and the meso-β-scale model of Richard *et al.* (1987). Apart from differences in the numerical techniques used, these two models differ essentially by the parameterization of soil and vegetation. In PERIDOT a simple two-temperature two-reservoir parameterization is used following Deardorff (1977), but is currently improved to account for stomatal resistance, root extraction and rainfall interception by vegetation. In the Richard *et al.* model, a more sophisticated approach is used as moisture and temperature are computed at 7 levels distributed over the upper meter of soil, and as a layer of vegetation, including its own energy budget, is included, following Deardorff (1978). These two models have been applied using a $(43)^2$-gridpoint computational domain centered on the HAPEX-MOBILHY zone, and a horizontal grid size of 10 km. Both models are initialized and take their time-dependent horizontal

boundary conditions from the above described analysis scheme.

A first example of model simulations is given in figure 10, where the surface winds at 10 m predicted by PERIDOT for June 16, 1986, at 12 and 18 GMT are compared to the wind measurements from the PATAC network. Although there are some differences between model results and experimental data in the eastern part of the domain, the model is clearly able to capture the essential mesoscale variability of the wind field, including the change of regime between 12 and 18 GMT, leading to a massive entry of moist maritime air over the domain. Another assessment of the quality of the model forecast at 12 GMT is given by the aircraft measurements shown in figure 11. An interesting feature of the model forecast is the strong upslope circulation caused by the Pyrenees range. Although scarce information is available from direct measurements of the wind, this circulation is confirmed by the development of moderate convection over the mountain range (as could be clearly seen on satellite views taken on this day).

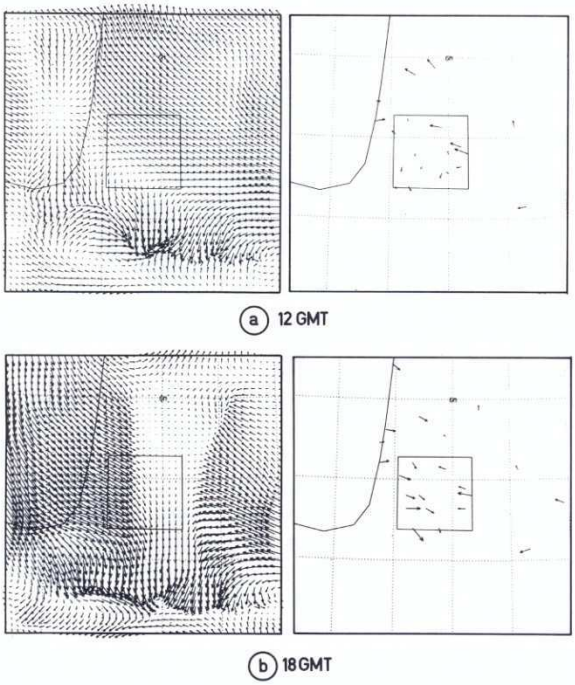

Figure 10

Comparison between surface winds as forecasted by the PERIDOT *mesoscale model at a height of* 18 m, *and observed at* 10 m *from the* PATAC *weather stations network, for June* 16, 1986, *at (a)* 12 GMT *and (b)* 18 GMT.

The main reason for implementing the numerical three-dimensional mesoscale models is to help in the derivation of spatially-integrated fluxes (see Section 5.1). The surface fluxes H and LE predicted by the PERIDOT model at 12 GMT average respectively 250 W m^{-2} and 350 W m^{-2} over the entire HAPEX-MOBILHY area. This corresponds roughly to the averaged values given by the SAMER stations, but is larger than the aircraft measurements (see table 3). It will be a major task in the near future to understand the reason(s) for such discrepancies, once better analyses of all existing data have been made. It should nevertheless be noted at this stage that the numerical models are able to reproduce quite well the atmospheric structure (wind and temperature three-dimensional fields), and that consequently they can be used

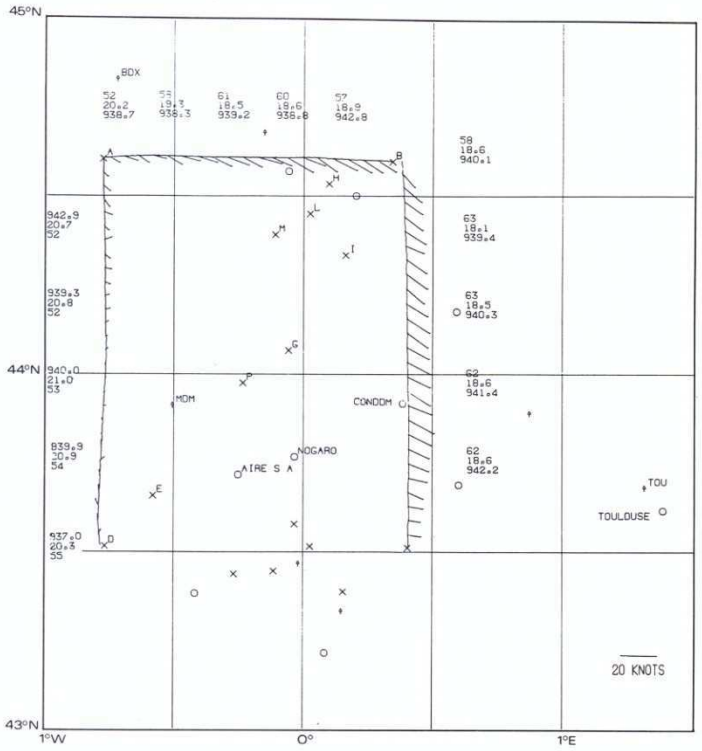

Figure 11

Boundary-layer winds observed from Piper-Aztec airplane around the experimental zone on June 16, 1986. *Wind vectors are shown ending on the limit of the experimental zone, which is also the flight track.*

Figure 12
Monthly averaged albedo from METEOSAT *for June* 1986.

with confidence as research tools to develop advanced parameterization schemes of area-averaged land-surface processes.

5.4. Implementation of detailed surface conditions

A necessary step to improve the realism and accuracy of mesoscale models is to provide them with detailed and spatially-varying surface conditions. This has to be done by prescribing for each grid element such parameters as the soil texture, the vegetation cover and the albedo. The former can be taken from previous geological and/or pedological surveys, but the latter two have to be specified from actual observations. Such mapping is presently under study, from either polar-orbiting or geostationary satellite information.

Figure 12 shows as an example the monthly averaged albedo which has been derived from METEOSAT data for June 1986, using the method proposed by Dedieu *et al.* (1987). One can note the low values corresponding to the pine forest in the northwestern part of the domain (see Section 3.2, and fig. 6) and the relatively higher values over the cultivated eastern part of the experimental zone. Another example is given in figure 13 which shows the Normalized Difference Vegetation Index (NDVI) estimated from NOAA-9 AVHRR data for May 22, 1986. Such a parameter allows for the mapping of vegetation types, as the orchard trees and vineyards are clearly seen in the valleys and as other types of canopies can be easily differentiated from each other. The NDVI varies from about 15 % for the pine forest and bare soils, to approximately 30 or 40 % for the cultivated areas.

It is expected that by including these surface conditions in the three-dimensional numerical mesoscale model, the accuracy and realism of the simulations will be greatly improved, and that it will be possible to achieve a better description of the surface fluxes and their spatial variations.

6. REMOTE SENSING STUDIES

The only feasible method for obtaining a data set on land-surface parameters and fluxes over the entire surface of the globe and to monitor them over long time periods is to use satellite observations. This is the task of the International Satellite Land-Surface Climatology Project (ISLSCP, Bolle and Rasool, 1985), which calls for satellite data collection and organization of ground-truth validation experiments. Among those, the remote-sensing part of the HAPEX-MOBILHY programme has served as the first trial for such an experiment. The HAPEX-MOBILHY remote-sensing studies have all been organized around the participation of the NASA C-130 instrumented aircraft (NASA/AMES, 1986), in conjunction with overpasses of various satellites (METEOSAT, NOAA, LANDSAT and SPOT), with three special objectives :

(*i*) calculation of surface moisture and heat fluxes using combined aircraft observations of surface temperature and soil moisture ;

(*ii*) spatial integration of aircraft surface albedo and temperature for comparison with satellite data ;

(*iii*) comparison of the fluxes estimated using the remotely-sensed data with those determined from the NCAR airborne eddy-correlation system.

6.1. The NASA C-130 operations and the inhomogeneity of surface conditions

To satisfy the above three objectives, different flight tracks have been flown for the C-130, ranging from low (300 m) and mid (1500 m) altitude passes over the two intensive test sites of Lubbon (sites # 1 and # 5) and Castelnau (site # 10) for objective (*i*), to high (6 km) altitude satellite underflights following north-

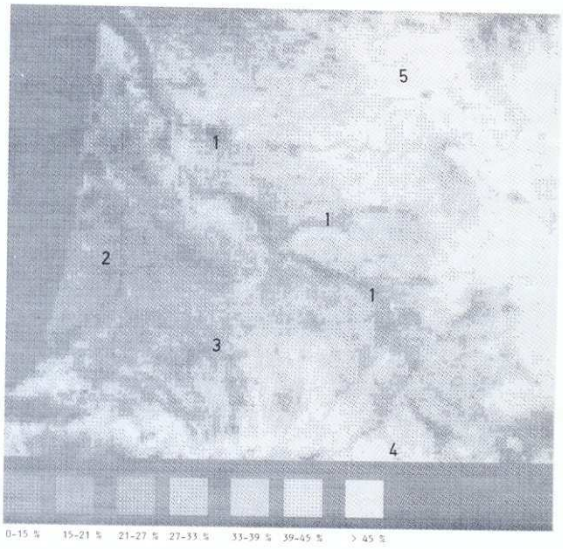

Figure 13
Normalized Difference Vegetation Index (NDVI) *for May* 22, 1986, *derived from* NOAA 9 AVHRR : 1 = *orchard trees and vineyards ;* 2 = *Landes forest ;* 3 = *corn and bare soil ;* 4 = *Pyrenees forest ;* 5 = *Limousin.*

Table 4
Sensors on board the NASA C-130 *remote sensing aircraft.*

PRT-5 —	8 - 14 Micron non-scanning radiometer, 2° FOV. On all flights.
NS001 —	Multispectral scanning visible to thermal IR radiometer, 8 spectral channels, 2.5 mrad IFOV, 100° FOV. The channels are at the following wavelengths (in microns) : 0.46 - 0.52, 0.53 - 0.60, 0.63 - 0.70, 0.77 - 0.91, 1.13 - 1.35, 1.57 - 1.71, 2.1 - 2.38, and 10.9 - 12.3. On all flights. This sensor is also known as the Thematic Mapper simulator. (Note the thermal channel on this sensor was not operable during HAPEX).
TIMS —	Multispectral scanner with 6 thermal IR channels, 2.5 mrad IFOV, 77° FOV. The channels are at the following wavelengths (in microns) : 8.2 - 8.6, 8.6 - 9.0, 9.0 - 9.4, 9.4 - 10.2, 10.2 - 11.2, and 11.2 - 12.2. On all flights after 3 June.
PBMR —	4-beam microwave radiometer at 21-cm wavelength, 0.25 rad IFOV. On all 300 and 1500 m flights.
CAMERA —	Metric, 9 inch color IR film, 6 inch focal length lens. On 9 and 16 June flights only.

south flight lines between the two above sites for objective (*ii*), and to coordinated 65 km flight lines flown at 1500 m for the C-130 and at 100 m for the King-Air for objective (*iii*).

The sensors and a brief description of their characteristics are listed in table 4. These sensors covered the wavelength region from the long wavelength 21 cm microwave radiometer to the visible wavelength of the NS-001 multispectral scanner. Figure 14 shows the spatial coverage of all the sensors in terms of the aircraft altitude H.

With a spatial resolution of the TIMS instrument of about 5 m, corresponding to a flight altitude of 1000 to 1500 m, it is possible to access the distribution of surface temperature at the small scale. As an example, temperature was found to vary by 10 to 12 K over the oat field of site # 1, these variations resulting from plant stress and being a possible indication of the underlying moisture availability. A histogram of the data for a 320 by 400 m^2 section (i.e. 3000 pixels) of the oat field in site # 1 is shown in figure 15. This broad spread of temperature has a standard deviation of 3 K. For comparison, figure 15 also shows the result for the corn field at site # 10 in Castelnau on the same day. There is a much more uniform temperature structure for the field, a 4 K spread and less than 1 K standard deviation. This field was much hotter with

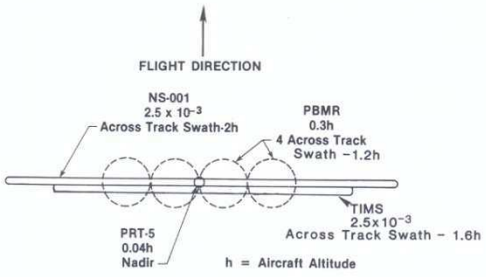

Figure 14
Schematic diagram of the spatial coverages for the sensors of the remote-sensing C-130 *aircraft.*

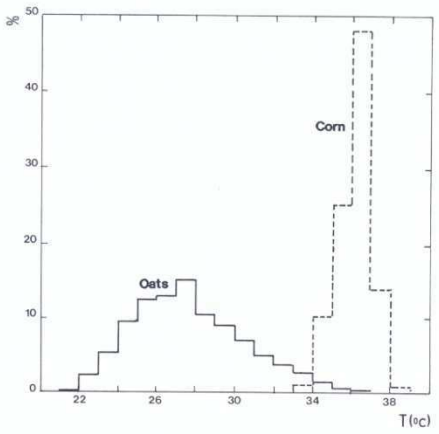

Figure 15
Histograms of the channel 6 *brightness temperatures on June* 23, 1986, *from an altitude of* 1200 m *over the oat field of Lubbon (site* # 1, *full line) and the corn field of Castelnau (site* # 10, *dashed line).*

smaller variations, indicating a uniformly dryer soil moisture condition. Such large spatial variability is also present at still smaller scales. For instance figure 16 shows the ground thermal infrared temperature for a square meter of the oat field in site # 1. The range of temperature is 3 K about the mean of about 25 °C over an area which was smaller than the aircraft pixel size. Particular attention will consequently have to be given to the spatial variability of the various parameters at the pixel scale, with special care to be paid to the effects of non-linearities : a comparison will be made between the fluxes obtained when the radiances are first integrated from small to large pixels and those obtained by integrating the fluxes from the small pixels over a larger area. All these integrated fluxes will then have to be compared with those determined with the NCAR King-Air eddy-correlation system.

Other effects may also play an important role for remote-sensing data interpretation and processing. Since there are 6 channels on the TIMS, it is possible to study the spectral response for the brightness temperature for a number of different target areas, such as for instance the cool and hot spots in the oat and corn fields in Lubbon and Castelnau. This is shown in figure 17 which shows considerable variation for the warmer targets, almost 10 K, indicating that there are some atmospheric effects which will have to be accounted for. The sharp variation between channels 3 and 4 for the corn fields may come from a spectral variation in the emissivity of the soil which is visible through the still sparse canopy.

6.2. Ground-truth vegetation measurements

At the same time that infra-red and micro-wave temperatures are collected by airborne remote-sensing, and surface-based flux-measuring systems provide estimates of the sensible H and latent LE heat fluxes, it is of importance to measure directly the various canopy parameters, such as the leaf area index (LAI), the foliage stomatal resistance and the leaf potential.

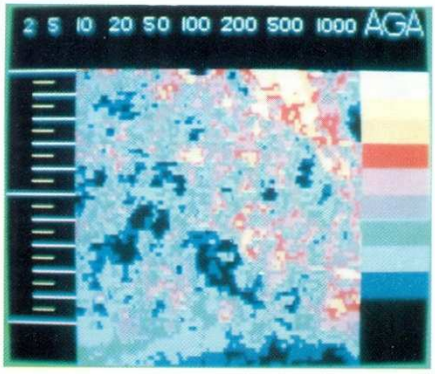

Figure 16
Small-scale variations of the infrared brightness temperatures over a 1 m^2 *area of oats at Lubbon (site* # 1*) on June* 16, 1986 ; *the average temperature is* 25 °C *and the range is* 3 K *(provided by courtesy of M. P. Stoll and F. Nerry, GSTS, Strasbourg).*

These parameters are indeed necessary to determine the « bulk canopy resistance », which allows for relating the surface fluxes to the afternoon surface temperature over dense vegetation (Taconet *et al.*, 1986*a*).

The influence of vegetation, and particularly of the phenological state of the agricultural canopies, on surface properties and consequently on evaporation fluxes as determined by remote-sensing techniques, can clearly be assessed from inspection of figure 18. The infra-red temperature as seen by the TIMS sensor varies indeed from 21 °C over the oat field in site # 1 (dark zone in the upper right-hand corner) to slightly more than 30 °C over the corn field of site # 5 (clearer zones in the left-hand part of the picture).

Results of the corresponding ground-truth measurements over vegetative canopies are shown in figure 19, where the monthly evolution of the mean stomatal resistance is taken on the same part of the upper corn leaves of the field in site # 5. One can further note in figure 19 the effects of irrigation, with an accompanying variation in resistance. Other measurements were taken during the SOP, namely the « basic potential » of leaves at dawn, which is a good indicator of the amount of water within the rooting zone, and the soil moisture tension in the upper 40 cm layer by gypsum

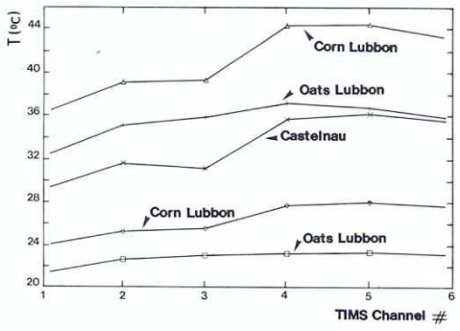

Figure 17
Plot of TIMS *spectral response for a variety of targets at both Lubbon (site* # 1*) and Castelnau (site* # 10*) for June* 23, 1986, *from an altitude of* 1200 m.

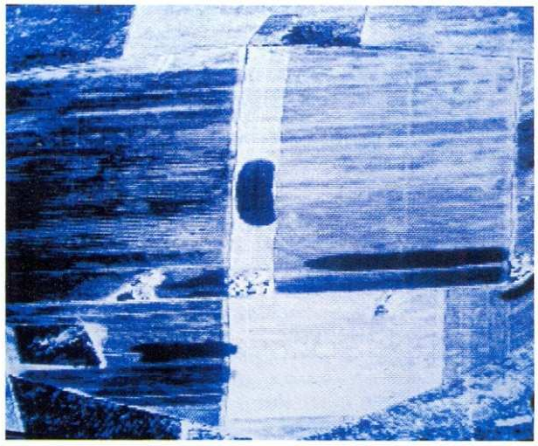

Figure 18
TIMS *channel* 5 *image over the Lubbon central site (sites* # 1 *and* 5*) from an altitude of* 1200 m *on June* 23, 1986, *at* 12 GMT (*the spatial resolution is approximately* 5 m).

block measurements. Taken altogether, these measurements of vegetation properties should allow for a better tuning and validation of transfer schemes used for the retrieval of surface fluxes from airborne, and later on from spaceborne, remote-sensing radiance measurements (see e.g. Carlson, 1985 ; Raffy and Becker, 1985 ; Taconet *et al.*, 1986*b*).

6.3. An example of surface fluxes determination

As a preliminary example showing the potential for estimating the surface fluxes H and LE from remote-sensing measurement of infra-red temperature, the method proposed by Jackson *et al.* (1977) and further developed by Seguin and Itier (1983), has been used for two days of the SOP, i.e. June 14 and 23, 1986. In this method, the surface energy budget, eq. (1), is rewritten using bulk-aerodynamic expressions for the surface fluxes, and reads after some algebra

$$T_s - T_a = \\ = ((R_N - G)\, h(V)/\rho C_p)(1 - LE/(R_N - G)) \quad (4)$$

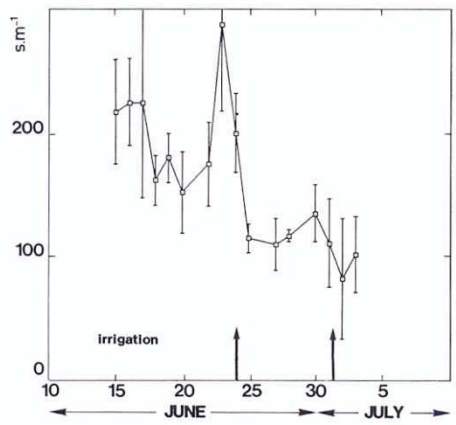

Figure 19
Time evolution of the stomatal resistance of the corn at Lubbon (site # 5*) during June* 1986.

where ρC_p is the air volumetric heat capacity and $h(V)$ is the inverse aerodynamic resistance. By measuring the difference $\Delta T = T_s - T_a$ between the surface and the air temperatures, one can consequently estimate LE if the net radiation R_N and the wind speed V are known.

Preliminary results from this method, assuming that $h(V)$ takes its value at neutrality and that $G = 0$, are shown in figure 20, where PRT5 measurements of surface temperature, PATAC measurements of wind and air temperature and SAMER measurements of net radiation and latent heat flux have been used for June 23, 1986, to calibrate the linear relation (4) between LE/R_N and $\Delta T = T_s - T_a$. This relation is then further used for the case of June 14, 1986, to infer LE from R_N as measured from the SAMER station and ΔT as measured from TIMS (channel 6) and PATAC wind and temperature. The comparison between calculated and measured fluxes is shown in table 5. It can be seen that there is a satisfactory agreement, especially if one keeps in mind that no corrections corresponding to either stability effects or emissivity influence were taken into account.

The surface latent and sensible heat fluxes will be further estimated from satellite remotely-sensed data, for example by using the diurnal cycle of surface temperature as inferred from METEOSAT radiances, following the method proposed previously by Wetzel *et al.* (1984). In a first stage this method will only be applied to retrieve the surface fluxes over agricultural crops and bare soil : it may indeed turn out to be of outmost difficulty to apply the method over very rough surfaces like the forested part of the experimental zone.

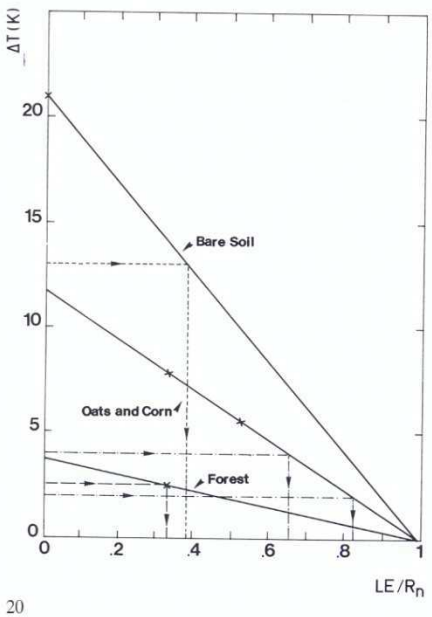

Figure 20

Parameterization of the normalized latent heat flux LE/R_N as a function of the temperature difference between the air and the surface (crosses indicate values derived from PRT5 *and* PATAC *and* SAMER *measurements on June* 23, 1986, *while dashed lines connect temperature differences observed from* TIMS, PATAC *and* SAMER *to predicted fluxes for June* 14, 1986).

Table 5

Surface fluxes of latent heat LE over various canopies at the central site for June 14, 1986, as measured from the SAMER *and Hydra stations and as estimated from remote-sensing measurements of the temperature difference between the air and the surface (see eq.* (4)).

Site #	Type of crop	Latent heat flux LE (W m^{-2}) measured by the SAMER and Hydra stations	Latent heat flux LE (W m^{-2}) derived from remote-sensing
1	Oats	200	290
5	Corn	190	230
—	Forest	150	119

7. CONCLUSION AND PERSPECTIVES

Organizing and running for about two-and-a-half months the Special Observing Period (SOP) of the HAPEX-MOBILHY programme has been in itself an experiment in carrying out experiments of this type, as about 150 scientists, technicians and support people were present in the field and involved in the various parts of the observational studies. This has nevertheless proven to be necessary in order to collect the complete data set against which parameterization schemes for land-surface and evaporation processes at the scale of a GCM grid square will be tested and further developed (see WCRP, 1983).

All the data collected during the HAPEX-MOBILHY's SOP, corresponding in particular to either atmospheric structure, or surface energy budget (eq. (1)), or subsurface moisture depletion, have to be complemented by information about the surface hydrological balance (eq. (2)). This is achieved by running the three-dimensional hydrological model of Girard and Boukerma (1985). This model has been previously developed and tested for the period 1974 to 1982 against precipitation measurements at the rain-gage stations (see Section 1) and against run-off data collected at the 33 stream-gaging stations corresponding to the catchments present within the experimental domain. It is presently being run for the period 1985 to 1987, using as inputs detailed precipitation and evaporation measurements taken during the HAPEX-MOBILHY experiment, and providing as outputs the surface run-off with an horizontal resolution of 10 km and the moisture content in the upper three soil layers at the same resolution.

The complete database, including measurements collected during the SOP and the remaining part of the HAPEX-MOBILHY programme, as well as the hydrological information assimilated by hydrological modelling, will be available for distribution to interested scientists by mid-1988. It will be provided at no cost other than the reproduction fees. These data are of great interest for intercomparison exercises, as the ones proposed by the World Climate Research Programme for either land-surface processes or boundary-layer codes (WCRP, 1987). It is hoped that this data set will prove of importance for the development of better parameterization schemes of evaporation over land surfaces, a primary goal of many climate and mesoscale modellers.

Acknowledgments

Many persons and agencies have been vital to the development of the HAPEX-MOBILHY programme. It is a pleasure to particularly thank P. Morel (WCRP & PNEDC), R. Serafin (NCAR), R. Murphy (NASA), M. Glass (PNEDC & INSU), and J. Labrousse and C. Pastre (DMN), who have made possible a number of important decisions. Thanks are also due to all of our colleagues who either participated in the field programme, or helped with its preparation.

Funding has been provided partly by the participating agencies, i.e. Direction de la Météorologie Nationale, Institut National de Recherches Agronomiques, National Aeronautics and Space Administration, National Science Foundation (grants ATM-8511196, ATM-8512535, INT-8514251, ATM-8601115) and National Center for Atmospheric Research, and United States Department of Agriculture. Additional funding has been provided under many grants : among others, Programme National d'Etude de la Dynamique du Climat (PNEDC 1984, 1985 and 1986), Institut National des Sciences de l'Univers (PAM 905624 and 905665), Programme Interdisciplinaire de Recherche sur l'Environnement Naturel (PIREN 508632), Centre National d'Etudes Spatiales (86/CNES/1285), Centre National de la Recherche Scientifique (DRCI 86/920118) and Commission of the European Communities (ST2J-0049-1-F & ST2J-0049-2-UK).

REFERENCES

André, J. C., J. P. Goutorbe, and A. Perrier, HAPEX-MOBILHY, a hydrologic atmospheric pilot experiment for the study of water budget and evaporation flux at the climatic scale, *Bull. Am. Meteorol. Soc.*, **67,** 138-144, 1986.

André, J. C., and Ph. Bougeault, On the use of the HAPEX-MOBILHY data for the validation and development of parameterization schemes of surface fluxes. *Report of the second session of the scientific steering group on land-surface processes and climate,* World Meteorological Organization, WCP126, Geneva, Switzerland, in press, 1987.

Bolle, H. J., and S. I. Rasool, (Eds.), Development of the implementation plan for the International Satellite Land-Surface Climatology Project (ISLSCP), Phase I, *World Meteorological Organization, WCP94,* Geneva, Switzerland, 56 pp., 1985.

Carlson, T. N., Regional-scale estimates of surface moisture availability and thermal inertia using remote thermal measurements, *Rem. Sens. Rev.*, **1,** 197-247, 1985.

Deardorff, J. W., A parameterization of ground surface moisture content for use in atmospheric prediction models, *J. Appl. Meteorol.*, **16,** 1182-1185, 1977.

Deardorff, J. W., Efficient prediction of ground temperature and moisture with inclusion of a layer of vegetation, *J. Geophys. Res.*, **83,** 1889-1903, 1978.

Dedieu, G., P. Y. Deschamps, and Y. M. Kerr, Satellite estimation of solar irradiance at the surface of the earth and of surface albedo using a physical model applied to METEOSAT data, *J. Clim. Appl. Meteorol.*, **26,** 79-87, 1987.

Durand, Y., The use of satellite data in French high resolution analysis, *ECMWF Workshop on high resolution objective analysis,* June 24-26 1985, 89-127 (available from ECMWF, Shinfield Park, Reading, Berkshire RG29AX, UK), 1985.

Gash, J. H. C., Observations of turbulence downwind of a forest-heath interface, *Bound.-Layer Meteorol.*, **36,** 227-237, 1986.

Girard, G., and B. Boukerma, Projet HAPEX-MOBILHY, calage du modèle hydrologique, exploitations spécifiques et propositions d'utilisation, *Rapport LHM/RD/85/110,* Centre d'Informatique Géologique (available from CIG, 35 rue Saint-Honoré, 77305 Fontainebleau Cedex, France), 1985.

Imbard, M., A. Joly, and R. Juvanon du Vachat, Le modèle de prévision numérique PERIDOT : Formulation dynamique et modes de fonctionnement, *Note EERM,* 161, 70 pp. (available from EERM, 73 rue de Sèvres, 92100 Boulogne, France), 1986.

Itier, B., Révision d'une méthode simplifiée pour la mesure du flux de chaleur sensible, *J. Rech. Atmos.*, **16,** 85-90, 1982.

Jackson, R. D., R. J. Reginato, and S. B. Idso, Wheat canopy temperature : A practical tool for evaluating water requirements, *Water Resour. Res.*, **13,** 651-656, 1977.

Llyod, C. R., W. J. Shuttleworth, J. H. C. Gash, and M. Turner, A microprocessor system for eddy correlation, *Agric. For. Meteorol.*, **33,** 67-80, 1984.

Mercusot, Ch., Ph. Bougeault, and Y. Durand, Programme HAPEX-MOBILHY, Atlas des analyses PERIDOT (available from Centre National de Recherches Météorologiques, 31057 Toulouse Cedex, France), 1986.

NASA/AMES, C-130B aircraft experimenters handbook. Medium-altitude Missions Branch, NASA/AMES Research Center (available from NASA/AMES, Medium-altitude Missions Branch, Moffett Field, Ca 94035, USA), 1986.

NCAR/RAF, The King-Air, Overview and summary of capabilities, *Research Aviation Facility Bull.*, **14,** 12 pp. (available from the National Center for Atmospheric Research, P. O. Box 3000, Boulder, Co 80307, USA), 1984.

Perrier, A., B. Itier, J. M. Bertolini, and A. Blanco de Pablos, Mesure automatique du bilan d'énergie d'une culture : Exemples d'applications, *Ann. Agron.*, **26,** 19-40, 1975.

Raffy, M., and F. Becker, An inverse problem occurring in remote sensing in the thermal infrared bands and its solution, *J. Geophys. Res.*, **90,** 5809-5819, 1985.

Richard, E., N. Chaumerliac, J. F. Mahfouf, and E. C. Nickerson, Numerical simulation of orographic enhancement of rain with a mesoscale model, *J. Climate Appl. Meteorol.*, **26,** 661-669, 1987.

Riou, Ch., Une expression analytique du flux de chaleur sensible en conditions suradiabatiques à partir de mesures du vent et de la température à deux niveaux, *J. Rech. Atmos.*, **16,** 15-22, 1982.

Seguin, B., and B. Itier, Using midday surface temperature to estimate daily evaporation from satellite thermal IR data, *Int. J. Rem. Sens.*, **4,** 371-383, 1983.

Shuttleworth, W. J., J. H. C. Gash, C. R. Lloyd, C. J. Moore, J. Roberts, A. de O. Marques, G. Fisch, V. de P. Silva, M. N. G. Ribeiro, L. C. B. Molion, L. D. A. de Sa, J. C. Nobre, O. M. R. Cabral, S. R. Patel, and J. C. de Moraes, Eddy correlation measurements of energy partition for Amazonian forest, *J. Roy. Meteorol. Soc.*, **110,** 1143-1162, 1984.

SMIRSO, PATAC : Rapport sur l'état d'avancement du projet au 31 Mai 1985, *Rapport Interne du SMIRSO* (available from Service Météorologique Inter-Régional du Sud-Ouest, BP 5, 33705 Mérignac, France), 1985.

Stull, R. B., On the ability of NCAR instrumented aircraft to measure turbulent humidity fluctuations, *Internal Report, Department of Meteorology, University of Wisconsin* (available from University of Wisconsin, Department of Meteorology, 1225 West Dayton Street, Madison, Wc 53706, USA), 1985.

Taconet, O., R. Bernard, and D. Vidal-Madjar, Evapotranspiration over an agricultural region using a surface flux/temperature model based on NOAA-AVHRR data, *J. Clim. Appl. Meteorol.*, **25,** 284-307, 1986a.

Taconet, O., T. Carlson, R. Bernard, and D. Vidal-Madjar, Evaluation of a surface/vegetation parameterization using satellite measurements of surface temperature, *J. Clim. Appl. Meteorol.*, **25,** 1752-1767, 1986b.

WCRP, Report of a meeting of experts on the design of a pilot atmospheric-hydrological experiment for WCRP, *World Meteorological Organization, WCP76,* Geneva, Switzerland, 45 pp., 1983.

WRCP, Report of the second session of the scientific steering group on land-surface processes and climate. *World Meteorological Organization, WCP126,* Geneva, Switzerland, in press, 1987.

Weill, A., F. Baudin, J. P. Goutorbe, P. Van Grunderbeeck, and P. Le Berre, Turbulence structure in temperature inversion and in convection fields as observed by Doppler sodar, *Bound.-Layer Meteorol.*, **15,** 375-390, 1978.

Weill, A., C. Klapisz, B. Strauss, F. Baudin, C. Jaupart, P. Van Grunderbeeck, and J. P. Goutorbe, Measuring heat flux and structure functions of temperature fluctuations with an acoustic Doppler sodar, *J. Appl. Meteorol.*, **19,** 199-205, 1980.

Wetzel, P. J., D. Atlas, and R. M. Woodward, Determining soil moisture from geosynchroneous satellite infrared data, A feasibility study, *J. Clim. Appl. Meteorol.*, **23,** 375-391, 1984.